Optics Letters

High-power, widely tunable, green-pumped femtosecond BiB_3O_6 optical parametric oscillator

Wenlong Tian,[1,2] Zhaohua Wang,[2,*] Xianghao Meng,[2] Ninghua Zhang,[1] Jiangfeng Zhu,[1] and Zhiyi Wei[2,3]

[1]School of Physics and Optoelectronic Engineering, Xidian University, Xi'an 710071, China
[2]Beijing National Laboratory for Condensed Matter Physics, Institute of Physics, Chinese Academy of Sciences, Beijing 100190, China
[3]e-mail: zywei@iphy.ac.cn
*Corresponding author: zhwang@iphy.ac.cn

Received 12 July 2016; revised 13 September 2016; accepted 17 September 2016; posted 21 September 2016 (Doc. ID 270324); published 17 October 2016

We report on an efficient high-power, widely tunable femtosecond optical parametric oscillator in BiB_3O_6, synchronously pumped by a frequency-doubled mode-locked Yb:KGW laser at 515 nm. Using collinear type I ($o \rightarrow e + e$) phase matching, a resonant wavelength range of 688–1057 nm at a 151-MHz repetition rate is demonstrated, with a tunable idler range of 1150–1900 nm. The output power at 705 nm is 1.09 W for 3.6 W pump power exceeding 30% conversion efficiency. Near-transform-limited pulses down to 71 fs are achieved by deploying extracavity dispersion compensation in a pair of SF6 prisms.

OCIS codes: (190.7110) Ultrafast nonlinear optics; (190.4970) Parametric oscillators and amplifiers; (190.4400) Nonlinear optics, materials.

http://dx.doi.org/10.1364/OL.41.004851

High-power, high-repetition-rate femtosecond pulses in the region of 700–1000 nm are of great interest for a variety of applications, such as biophotonics, time-resolved spectroscopy, and optical frequency combs [1–3]. Ti:sapphire laser, as the workhorse for so long [4,5], can generate more than 1 W average power, with broadband spectrum or tunable wavelength over 700–1000 nm; however, it costs a lot and produces sub-100 fs pulses only around 800 nm. Another attractive alternative approach that has been promoted recently is the femtosecond optical parametric oscillators (OPOs) synchronously pumped by the second harmonic generation (SHG) of Yb:fiber amplifiers or high-power bulk-oscillators. Based on this kind of OPO, widely tunable signals ranging from 600 to 1000 nm with both watt-level output power and sub-100 fs pulse duration are expected to be obtained. Currently, due to the periodically poled nonlinear crystals such as periodically poled lithium niobate (PPLN) or periodically poled stoichiometric lithium tantalate (PPsLT) having much larger dispersion properties as well as a smaller damage threshold in the visible region, the most common nonlinear crystals for the green-pumped femtosecond OPO were β-BaB_2O_4 (BBO) or LiB_3O_5 (LBO). In 2011, Cleff *et al.* reported a femtosecond OPO based on LBO pumped by a frequency-doubled Yb:fiber amplifier at 525 nm, providing signals tuning over 780–940 nm with the maximum output power of 250 mW [6]. Based on a noncollinear BBO OPO pumped by the SHG of a femtosecond Yb:$KLu(WO_4)_2$ thin-disk oscillator, Lang *et al.* generated ultrawidely tunable femtosecond pulses over 600–1200 nm with more than 3 W maximum average power in 2012 [7]. In 2013, Gu *et al.* implemented the intracavity SHG and sum frequency generation (SFG) in an Yb:fiber laser pumped OPO, generating femtosecond pulses over 610–668 nm for SFG and 716–970 nm for SHG with 23.5% conversion efficiency [8]. They also realized a dual-wavelength femtosecond LBO OPO covering the visible and near-infrared (NIR) wavelength over 555–623 nm and 658–846 nm pumped by a frequency-doubled Yb:fiber laser in 2014 [9]. Most recently, Vengelis *et al.* investigated the characteristics of femtosecond OPOs based on both LBO and BBO, synchronously pumped by the SHG of a femtosecond Yb:KGW laser [10].

Other than BBO and LBO, BiB_3O_6 (BIBO) is another excellent candidate with unique optical properties for frequency conversion applications in the visible to NIR. The BIBO crystal combines the advantages of UV transparency and high optical damage threshold with substantially larger optical nonlinearity. While BIBO has larger group velocity dispersion in the visible and NIR range than BBO and LBO crystals, it has great advantages in high-power green-pumped femtosecond OPO. First, BIBO offers versatile phase-matching properties and flexible wavelength-tuning characteristics, with an effective nonlinear coefficient as high as 3.7 pm/V [11], which is nearly twice and four times larger than those of BBO and LBO, respectively. Second, both the BBO and LBO crystal possess two couples of signal/idler for every single phase matching angle, which makes it easy for them to generate dual-wavelength signal operation under high-power pumping. This does not happen in a green-pumped BIBO OPO. As a biaxial crystal, BIBO also offers large angular and spectral acceptance bandwidth, low spatial walk-off, and broadband angle tuning at room temperature. It is also not hygroscopic and is readily available in high optical

quality, in large size, and at low cost [12]. Up to now, several studies on nonlinear frequency conversion including femtosecond OPO, SHG, and optical parametric amplification have been reported [13–16].

In this Letter, we report on an efficient high-power femtosecond BIBO OPO pumped by a 515 nm femtosecond green source for the first time. Using 1-mm-long BIBO and deploying type I ($o \rightarrow e + e$) phase matching, we obtain widely tunable resonant pulses from 688 to 1057 nm at 151 MHz by angle tuning. The maximum output power is as high as 1.09 W with a fluctuation less than 2% rms over 1 h for 3.6 W pump power. We use a pair of SF6 prisms for extracavity dispersion compensation and realize the near-transform-limited pulses with duration down to 71 fs. By replacing the output coupler with a flat high-reflectivity mirror, idlers across 1150 to 1900 nm with the maximum average power of 414 mW are also generated.

The schematic of the experimental setup is shown in Fig. 1. The pump source is a commercial Kerr-lens mode-locked Yb:KGW laser (Light Conversion, FLINT6.0) delivering 90 fs pulses at 1030 nm with up to 6.8 W average power. The repetition rate of the Yb:KGW laser is 75.57 MHz, corresponding to the linear cavity length of 1983.5 mm. The fundamental wave is focused by a lens (L1, $f = 75$ mm) into a 2.5-mm LBO crystal cut at $\theta = 90°$ and $\varphi = 13.6°$ for type I ($e \rightarrow o + o$) SHG, whose two surfaces are both antireflection coated at both 1030 and 515 nm wavelengths. A half wave plane (HWP) at 1030 nm was used to control the polarization of the fundamental wave. The generated second harmonic wave centered at 515 nm had as large as 4.1 W average power and was collimated with the second lens (L2, $f = 150$ mm). The optical spectrum of the SHG pulses is also depicted in Fig. 1. We used four dichroic mirrors (DMs) to separate the second harmonic and the fundamental wave. To control the power and polarization of the second harmonic radiation, an attenuator consisting of two HWPs and a polarization beamsplitter (PBS) was used. The second harmonic wave was focused into the BIBO crystal using a lens (L3, $f = 150$ mm). Due to the loss from the DMs and the lenses, the maximum power after L3 was 3.6 W.

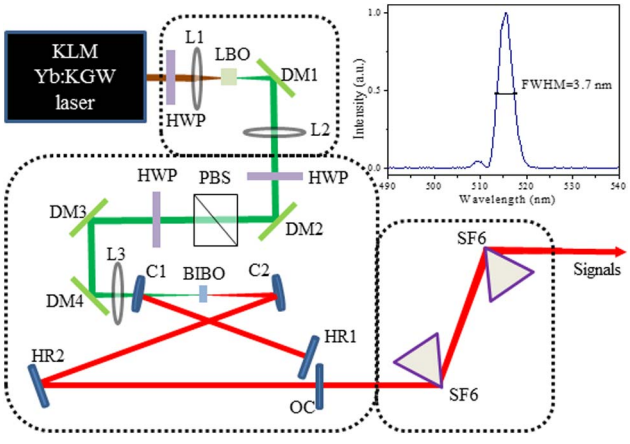

Fig. 1. Sketch for the experimental setup of the femtosecond OPO based on a BIBO. HWP: half wave plate; DM1–DM4: dichroic mirrors; PBS: polarization beamsplitter; L1–L3: lenses; HR1–HR2: high-reflectivity flat mirrors; OC: output coupler; C1 and C2: concave mirrors; SF6: prism. Inset: optical spectrum of the SHG pulses.

The signal single resonant OPO was a linear standing wave cavity with five mirrors, whose repetition rate was set to be 151 MHz, corresponding to twice of that of the pump laser. C1 was a concave mirror with 150 mm radium of curvature (ROC), coated with high reflectively over 620–1080 nm ($R > 99.9\%$), and high transmittance around 488–532 nm ($R < 5\%$). A concave mirror with ROC of 100 mm (C2) and two flat mirrors (HR1 and HR2) were not only coated with high reflectivity over 620–1120 nm ($R > 99.9\%$) but were also group delay (GD) optimized. The output coupler (OC), which was mounted on a translation stage for finely tuning the cavity length, had 11% transmittance at the range of 640–1050 nm and was GD dispersion optimized. The BIBO crystal was cut at $\theta = 174°$ and $\varphi = 90°$ for type I ($o \rightarrow e + e$) phase matching in the $y - z$ plane and coated with high transmittance in both the 510–530 and 700–1040 nm regions. Taking the material dispersion and the group velocity mismatching between pump and signals of the BIBO crystal into consideration, here we used a 1-mm-long BIBO crystal. The beam waist radius in the center of the BIBO was calculated to be 23 μm based on the ABCD matrix. The corresponding spatial walk-off length and the maximum incident angle for such 1-mm-long BIBO crystals were 11.79 μm and 9.3 mrad, respectively, which were much smaller than the waist diameter of both signal and pump as well as the acceptable angular of 33.2 mrad. Therefore, they would have little effect on the OPO performance. In addition, the average temporal walk-off between the signals from 650 to 1030 nm and pump of 515 nm for 1-mm-long BIBO crystal was 134 fs. While this would have some implications on the pulse duration of signal pulses, a pair of prisms (SF6) was employed to compensate the dispersion outside the cavity. The extracavity dispersion compensation would also reduce the difficulty for pre-alignment of the cavity over intracavity dispersion compensation using a prism pair.

The OPO cavity was aligned with the green laser easily, and then the parametric oscillation was achieved by finely tuning the cavity length to meet the synchronous pumping condition. After fine alignment, the maximum output power of 1.09 W at the fundamental transverse mode (TEM_{00}) for 3.6 W pump power was obtained when the pump laser was normally incident into the BIBO crystal, resulting in the maximum gain and minimum loss. The corresponding signal was 705 nm. Figure 2 shows the dependence between the output power and the pump power.

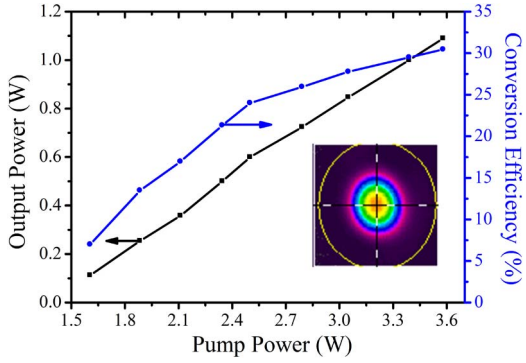

Fig. 2. Output power (black) and the corresponding conversion efficiency (blue) of the femtosecond OPO based on BIBO. Inset: beam profile at the maximum output power.

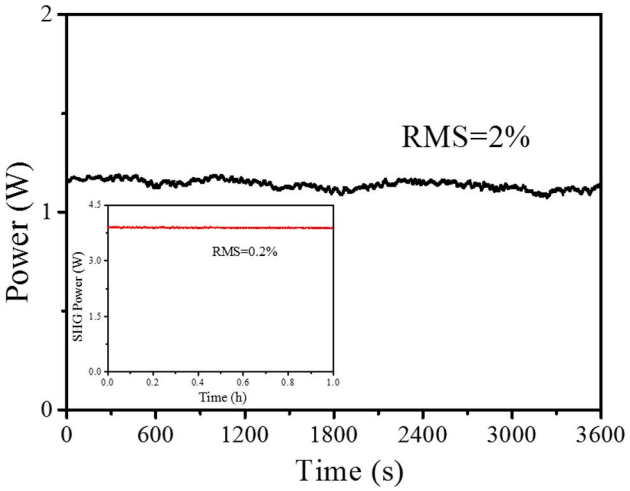

Fig. 3. Long-term power stability of the maximum output power from the femtosecond OPO based on BIBO. Inset: power stability of the pump power in 1 h.

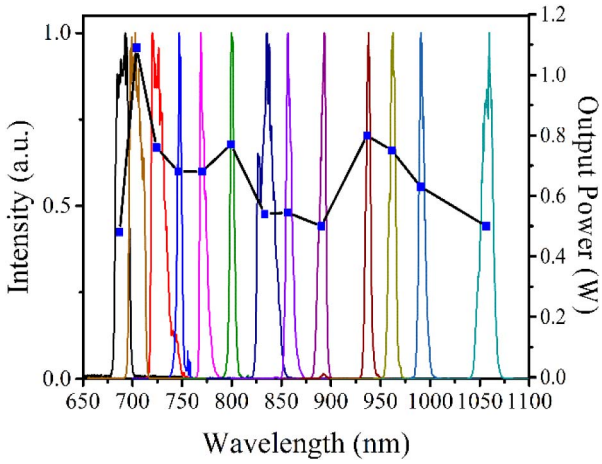

Fig. 4. Normalized output spectra and the corresponding average output power across the tuning range of the femtosecond BIBO OPO.

It is obviously to see that the output power was linearly increasing with the pump power, and the maximum conversion efficiency was about 30%. The beam quality (M^2) at the maximum output power was also measured with a commercial M^2 factor meter (Spiricon M^2 – 200 s), resulting in the M_X^2 and M_Y^2 being equal to 1.33 and 1.37, respectively. The beam quality factor was higher than that of the pump pulses ($M_X^2 = 1.19$ and $M_Y^2 = 1.10$), which originated from the astigmatism caused by two folded concave mirrors. The inset in Fig. 2 is the near-field beam profile at the maximum output power.

Then we performed the output stability by measuring the long-term average power fluctuation. For the fixed pump power of 3.6 W, the recorded power stability in 1 h is shown in Fig. 3. It can be seen that the output power was naturally stable with a fluctuation of 2% rms over 1 h. For comparison, we also give the corresponding power stability of pump power with only 0.2% rms fluctuation in 1 h, as inserted in Fig. 3. The dropping of power stability was believed to be derived from the ambient temperature fluctuation, air flow, and mechanical vibration, which can be effectively suppressed by isolation and active feedback control.

By changing the angle of BIBO, resonant pulses from 688 to 1057 nm were obtained, and their spectra were measured with a commercial optical spectrum analyzer (YOKOGAWA, AQ6370C), as shown in Fig. 4. It should be noticed that the resonant wavelength is beyond the signal wavelength limit (1030 nm), which can be attributed to the wider reflection coating range. The shortest wavelength of 688 nm in our experiment was limited by the phase-matching condition of the BIBO on the $y-z$ plane, and the longest wavelength of 1057 nm was limited by the coating of the C1 mirror (high reflectivity over 620–1080 nm). The maximum average powers at different resonant wavelengths are also depicted in Fig. 4. All the maximum average powers of the resonant pulses across the tuning range were above 450 mW.

For extracavity dispersion compensation, a pair of SF6 prisms with the tip–tip distance between the two prisms of 370 mm was employed. Fine dispersion control was managed by changing the insert length of the second prism. The pulse duration with dispersion compensation was in the range of 71 to 122 fs, measured by a commercial intensity autocorrelator (FR-103MN, Femtochrome Research, Inc.). Figure 5 shows the typical intensity autocorrelation trace and optical spectrum for signal at 850 nm. The full width at half-maximum (FWHM) bandwidth of the spectrum at 850 nm was 15 nm, and the corresponding transform-limited (TL) pulse duration was 52 fs, calculated by Fourier transforming the spectrum without dispersion. The autocorrelation width of the TL pulse was 79 fs, which was close to the measured value of 109 fs as shown in Fig. 5.

The idler performance was also characterized by replacing the output coupler with a flat high-reflectivity mirror and extracting the idlers directly from the behind of C2. The idler spectra were recorded from 1150 to 1900 nm with a commercial wavelength meter (WaveScan, A. P. E GmbH), as shown in Fig. 6. Figure 6 also depicts the output powers crossing the idler range. Because the surface of C2 was not coated with high transmittance in the idler range, the maximum average power of the idler was 414 mW with a rapid drop of power near

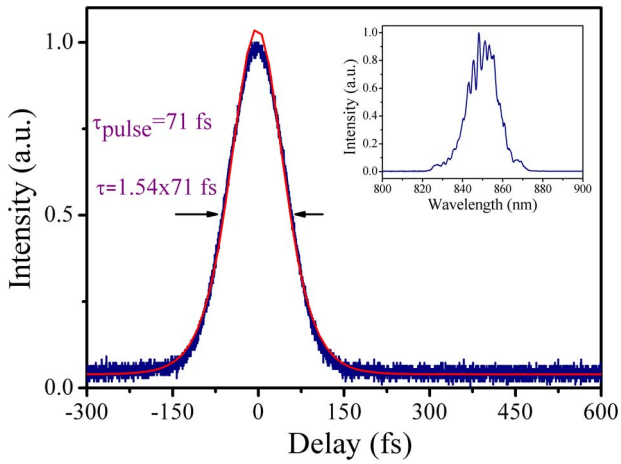

Fig. 5. Typical intensity autocorrelation trace with dispersion compensation for signal at 850 nm. Inset: the corresponding optical spectrum.

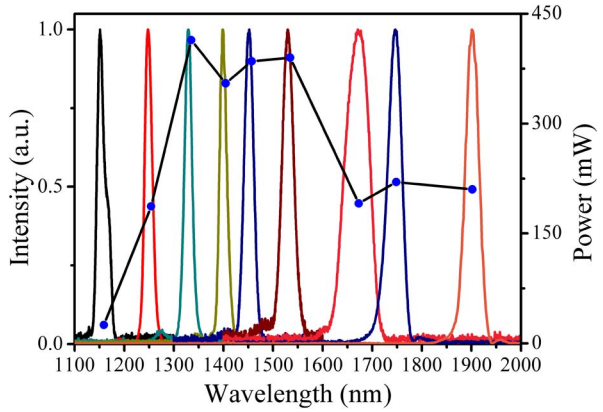

Fig. 6. Normalized idler spectra and the corresponding average powers across the tuning range of the femtosecond OPO.

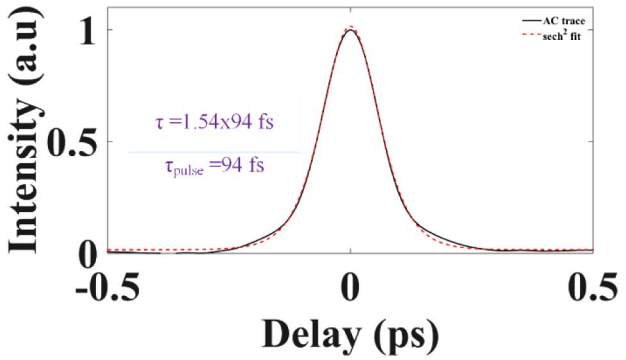

Fig. 7. Typical intensity autocorrelation trace for idler at 1670 nm: the solid trace is experimental data, and the red dot curve is the corresponding hyperbolic secant shape fitting.

1150 nm. This is because it is close to the edge of the coating of the C2 mirrors with high reflectivity over 620–1120 nm. The idler spectra seem to be a smooth Gaussian shape since they were single passing through the BIBO. The pulse durations over the tunable idler range were in the range of 94 to 223 fs, if hyperbolic secant shape pulses were assumed, measured by a commercial autocorrelator (PulseCheck-50, A. P. E. GmbH). Shown in Fig. 7 is the typical intensity autocorrelation trace of the 1670 nm idler whose spectrum is displayed in Fig. 6; the corresponding pulse duration is 94 fs.

In conclusion, we have reported on a femtosecond BIBO OPO synchronously pumped by the SHG of a Kerr-lens mode-locked Yb:KGW laser. Using an OC with 11% transmittance, the maximum output power of 1.09 W at 705 nm has been obtained, with a long-term average power fluctuation of 2% rms in 1 h. The signal conversion efficiency is 30%, and the total efficiency including the idler is 41.4%. By rotating the angle of the 1-mm-long BIBO, resonant wavelength covering from 688 to 1057 nm was realized, with the average power more than 450 mW for 3.6 W pump power. Using a pair of SF6 prisms for extracavity dispersion compensation, the shortest pulse duration was compressed down to 71 fs at 850 nm. Moreover, we have characterized the idler performance by replacing the OC with a high-reflective mirror. Idlers from 1150 to 1900 nm were obtained with the maximum output power of 414 mW. The typical pulse duration of the idler at 1670 nm was as short as 94 fs. Compared to previous works with BBO or LBO crystals [6–10], here we not only obtain the widest tunable pulses range from 688 to 1900 nm but also realize the highest parametric conversion efficient of 30% from pump to signal power. Future work will be focused on increasing the output power by refocusing the residual pump power and extending the operating wavelength by intracavity SHG and SFG processes. Such a high-power 100-fs widely tunable NIR femtosecond source is believed to be attractive in various applications such as time-domain spectroscopy and frequency metrology.

Funding. National Key Basic Research Program of China (2013CB922402); National Key Scientific Instruments Development Program of China (2012YQ120047); National Natural Science Foundation of China (NSFC) (11174361, 61575217, 61205130); Chinese Academy of Sciences (CAS) Key Deployment Project (KJZD-EW-L11-03).

Acknowledgment. We thank Dr. Shaobo Fang for useful discussion and manuscript revision.

REFERENCES

1. S. H. Chung and E. Mazur, J. Biophoton. **2**, 557 (2009).
2. M. Drescher, M. Hentschel, R. Kienberger, M. Uiberacker, V. Ya-kovlev, A. Scrinzi, T. Westerwal-besloh, U. Kleineberg, U. Heinz-mann, and F. Krausz, Nature **419**, 803 (2002).
3. A. Schliesser, N. Picque, and T. W. Hansch, Nat. Photonics **6**, 440 (2012).
4. Z. J. Yu, H. N. Han, L. Zhang, H. Teng, Z. H. Wang, and Z. Y. Wei, Appl. Phys. Express **7**, 102702 (2014).
5. A. Bartels, D. Heinecke, and S. A. Diddams, Opt. Lett. **33**, 1905 (2008).
6. C. Cleff, J. Epping, P. Gross, and C. Fallnich, Appl. Phys. B **103**, 795 (2011).
7. T. Lang, T. Binhammer, S. Rausch, G. Palmer, M. Emons, M. Schultze, A. Harth, and U. Morgner, Opt. Express **20**, 912 (2012).
8. C. L. Gu, M. L. Hu, L. M. Zhang, J. T. Fan, Y. J. Song, C. Y. Wang, and D. T. Reid, Opt. Lett. **38**, 1820 (2013).
9. C. L. Gu, M. L. Hu, J. T. Fan, Y. J. Song, B. W. Liu, and C. Y. Wang, Opt. Lett. **39**, 3896 (2014).
10. J. Vengelis, I. Stasevicius, K. Stankeviciute, V. Jarutis, R. Grigonis, M. Vengris, and V. Sirutkaitis, Opt. Commun. **338**, 277 (2015).
11. M. Ghotbi and M. E. Zadeh, Opt. Lett. **30**, 3395 (2005).
12. V. Petrov, M. Ghotbi, O. Kokabee, A. E. Martin, F. Noack, A. Gaydardzhiev, I. Nikolov, P. Tzankov, I. Buchvarov, K. Miyata, A. Majchrowski, I. V. Kityk, F. Rotermund, E. Michalshi, and M. E. Zadeh, Laser Photon. Rev. **4**, 53 (2010).
13. M. Ghotbi, M. Ebrahim-Zadeh, V. Petrov, P. Tzankov, and F. Noack, Opt. Express **14**, 10621 (2006).
14. A. E. Martin, O. Kokabee, and M. E. Zadeh, Opt. Lett. **33**, 2650 (2008).
15. A. E. Martin, V. R. Badarla, V. Petrov, and M. E. Zadeh, Opt. Lett. **36**, 1671 (2011).
16. A. Chaitanya, A. Aadhi, R. P. Singh, and G. K. Samanta, Opt. Lett. **39**, 5419 (2014).